Band discontinuities in $In_xGa_{1-x}As$-InP and InP-$Al_yIn_{1-y}As$ heterostructures: Evidence of noncommutativity

W. Seidel, O. Krebs, and P. Voisin
Laboratoire de Physique de la Matière Condensée de l'Ecole Normale Supérieure, 24 rue Lhomond, F 75005 Paris, France

J. C. Harmand, F. Aristone,* and J. F. Palmier
France-Télécom–Centre National d'Etudes des Télécommunications, 196 avenue Henri Ravera, 92225 Bagneux, France
(Received 14 March 1996)

We report on conduction-band offset measurements in InP-$In_{0.53}Ga_{0.47}As$ and InP-$Al_{0.48}In_{0.52}As$ heterostructures using internal photoemission, temperature-dependent current-voltage experiments, and photoluminescence excitation spectroscopy. The direct and inverse interfaces have been investigated separately. We find noncommutativity of 88 ± 10 meV for InP-$In_{0.53}Ga_{0.47}As$ and 53 ± 10 meV for InP-$Al_{0.48}In_{0.52}As$. We also find a significant nontransitivity for the average offsets in the InP-$Al_yIn_{1-y}As$-$In_xGa_{1-x}As$ family. These experimental results are in close agreement with recent theoretical predictions. [S0163-1829(97)01503-8]

The band offsets (BO) at semiconductor heterojunctions have an important impact on optical and electronic properties of heterostructures and are therefore a crucial parameter for the design of heterojunction devices. During the last decade, much effort has been spent in measuring and understanding band discontinuities.[1,2] Nevertheless, there is still a lot of recent interest in this field. The debate about deciding whether BO's are determined by bulk properties of the constituent materials or by interface-specific dipoles and strain effects is not closed. The former hypothesis[3–5] obviously implies band-offset transitivity and commutativity, whereas according to the latter one, both are not necessarily verified. The question of transitivity and commutativity has recently been studied in particular in the InP-$Al_yIn_{1-y}As$-$In_xGa_{1-x}As$ family of heterostructures, which is important for various applications like high-performance optoelectronic devices[6,7] for optical-fiber telecommunications. The results for these systems are controversial on both the experimental and theoretical sides. Transitivity is obtained (i) experimentally by Waldrop *et al.*[8] with x-ray photoemission spectroscopy and Böhrer *et al.*[9] with a combination of calorimetric-absorption spectroscopy and band-structure calculations, (ii) theoretically by Hybertsen[10] with first-principles calculations. In contrast, Lugagne-Delpon, André, and Voisin[11] found experimentally clear nontransitivity with photoluminescence (PL), photoluminescence excitation (PLE), and photocurrent (PC) measurements. While commutativity is found for the InP-$In_xGa_{1-x}As$ system by Dandrea and Duke[12] with first-principles calculations, noncommutativity was found (i) in the same system by Foulon and Priester[13] with self-consistent tight-binding treatment and experimentally by Landesman *et al.*[14] with ultraviolet photoemission spectroscopy, (ii) in InP-$Al_yIn_{1-y}As$ by Lugagne-Delpon, André, and Voisin[11] with PL, PLE, and PC. While transitivity has only a fundamental relevance, noncommutativity (asymmetry) also has important consequences for the optical properties of multiple quantum wells (QW's) or superlattices: in order to avoid the build-up of a macroscopic potential by summing the band-offset differences of each QW, the system has to create a built-in electric field by accumulating electric charges near the terminating planes.[15] This results in Stark shifts of the energy levels and occurrence of parity-forbidden transitions through symmetry breaking. Therefore, it is of interest to know, in particular for the InP-$In_xGa_{1-x}As$ system, whether the offsets are asymmetric or not, and by how much. Conversely, for $In_xGa_{1-x}As$-$Al_yIn_{1-y}As$, BO asymmetry can most likely be ruled out since the two materials share the same anion.[13] A further issue to be discussed is the possible dependence of the results on the growth process. Indeed, exchange mechanisms leading to segregation have been evidenced in several cases, like In segregation in $In_xGa_{1-x}As$-strained layers grown on GaAs.[16] Such processes are thermoactivated and depend on the growth kinetics. Hence, the atomic structure of the interface and possibly the band offset itself may depend on the growth conditions. This is likely the case in no-common atom systems like (InGa)As-InP or (AlIn)As-InP. Clearly, the question of band-offset transitivity and commutativity in the $In_xGa_{1-x}As$-$Al_yIn_{1-y}As$-InP family of heterostructures is still unclear and has technological importance in addition to its fundamental interest.

On the experimental side, the obvious lesson to be drawn from the past is that several qualitatively different measurements performed on well-characterized materials are necessary to get sufficient confidence. In this paper we report on BO determination in InP-$In_{0.53}Ga_{0.47}As$ and InP-$Al_{0.48}In_{0.52}As$ for both the direct (arsenide grown on phosphide) and inverse (phosphide grown on arsenide) heterojunctions separately. We used temperature-dependent current-voltage measurements (JVT) and in addition internal photoemission for InP-$In_{0.53}Ga_{0.47}As$. While the determination of the absolute BO's is accompanied with the usual uncertainties, differences between similar structures are very precise, because systematic modelization inaccuracies compensate mutually. In addition, we discuss PLE measurements in wide $In_xGa_{1-x}As$-InP QW's, which bring a convincing qualitative proof of the strong asymmetry of the potential well.

The experiments are performed on four samples grown by elemental-source molecular-beam epitaxy (MBE). The

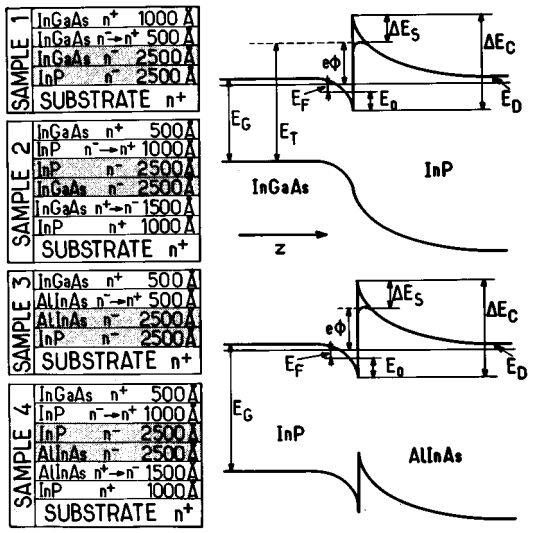

FIG. 1. The left column shows the sample structures. The low-doping concentration n^- is $\approx 10^{16}$ cm^{-3}, and the heavy doping n^+ is $\approx 2\times 10^{19}$ cm^{-3}. The right column shows schematically the band structure of the $In_xGa_{1-x}As$-InP and InP-$Al_yIn_{1-y}As$ interfaces. ΔE_c is the conduction-band offset, ΔE_s is the Schottky lowering, E_D is the donor binding energy, E_F is the Fermi energy, E_g is the $In_xGa_{1-x}As$ band gap, E_0 is the energy of the ground state of the band-bending potential well, $e\Phi$ is the activation energy, and E_T is the difference between the top of the effective potential barrier and the top of the $In_xGa_{1-x}As$ valence band.

group-V solid sources were loaded into valved cracking cells. The samples were grown at 500 °C on (001)-oriented n^+-type InP substrates. The corresponding growth sequences are shown on the left part of Fig. 1. Each sample forms a n^--n^- heterojunction between heavily n-doped substrate and contact layers. Sample 1 is the direct InP-$In_{0.53}Ga_{0.47}As$ interface ($In_{0.53}Ga_{0.47}As$ grown on InP): it consists of a 2500-Å InP buffer layer followed by a 2500-Å $In_{0.53}Ga_{0.47}As$ layer. Both layers have a light n-type doping $n_D=1\times 10^{16}$ cm^{-3}. To facilitate Ohmic contacts, a 500-Å $In_{0.53}Ga_{0.47}As$ gradual doping layer (where n_D increases from 10^{16} cm^{-3} to 2×10^{19} cm^{-3}) and a further 1000-Å $In_{0.53}Ga_{0.47}As$ layer ($n_D=2\times 10^{19}$ cm^{-3}) are added. Sample 2 represents the inverse interface (InP grown on $In_{0.53}Ga_{0.47}As$). To avoid the perturbation of the electrical measurements by the inevitable direct interface following the buffer layer, the corresponding layers have been heavily n-doped ($n_D=2\times 10^{19}$ cm^{-3}). The same has been done with the other direct interface between the InP contact layer and the $In_{0.53}Ga_{0.47}As$ cap layer. Samples 3 and 4 form the direct and inverse interface for InP-$Al_{0.48}In_{0.52}As$, respectively. They have been tailored likewise. Deep-etched 40-μm diodes with evaporated gold contacts have been processed for electrical measurements. Material composition and quality were assessed by PL and PLE. Good sample quality is evidenced by the narrow linewidths and small Stokes shifts, and nominal composition of the alloys is verified.

We first examine the JVT measurements. We have followed the approach proposed by Hickmott[17] and studied the activation energy governing current transport in the direction perpendicular to the heterojunction interface. The JV characteristic is described by the thermionic-emission theory,

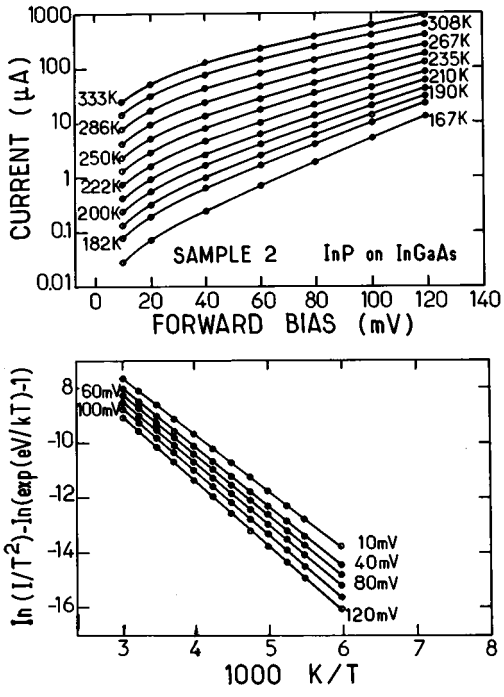

FIG. 2. Temperature-dependent U-I curves of sample 2 for forward bias, at various temperatures between 167 and 333 K, and Arrhenius plots derived from these data.

which relates the flux of carriers incident upon an interfacial barrier, with sufficient energy to overcome it, to the temperature T and the height of the barrier $e\phi$. The current density J is given by the approximate expression[18]

$$J=A^*T^2\exp(-e\phi/kT)\{\exp(eV/kT)-1\}, \qquad (1)$$

where V is the forward bias, A^* is the effective Richardson constant, e is the electron charge, T is the temperature, and k is the Boltzmann constant. A major advantage of these electrical measurements over those inherited from surface physics (like photoemission-based methods) is their insensitivity to the detail of the potential barrier shape, as soon as the interface sharpness is smaller than the electron mean-free path. As illustrated in Fig. 1(b), the potential barrier $e\phi$ is approximately equal to $\Delta E_c-\Delta E_s-E_F-E_0$, where ΔE_c is the conduction BO (CBO), E_0 is the ground level of the band-bending quantum well at the interface, E_F is the Fermi energy (measured from E_0), and ΔE_s is the Schottky lowering, associated with image forces. Rearranging Eq. (1) yields

$$\ln\{J/T^2\}-\ln\{\exp(eV/kT)-1\}=-e\phi/kT+\ln A^*. \qquad (2)$$

Thus, measuring the slope of $\ln\{J/T^2\}-\ln\{\exp(eV/kT)-1\}$ versus $1/T$ and interpolating to 0 V yields $e\phi$. The interpolation is also useful for eliminating bias-connected deviations from this simplified description, like bias-induced change of the band bending, etc. Note also that ΔE_c and the carrier density are assumed to be temperature independent.

The experiments have been performed with a variable-temperature cryostat from Oxford Instruments and a high sensitive Keithley amperemeter. The JV curves of sample 2 under forward bias, at various temperatures, are displayed in Fig. 2(a) and prove the thermoactivated character of the con-

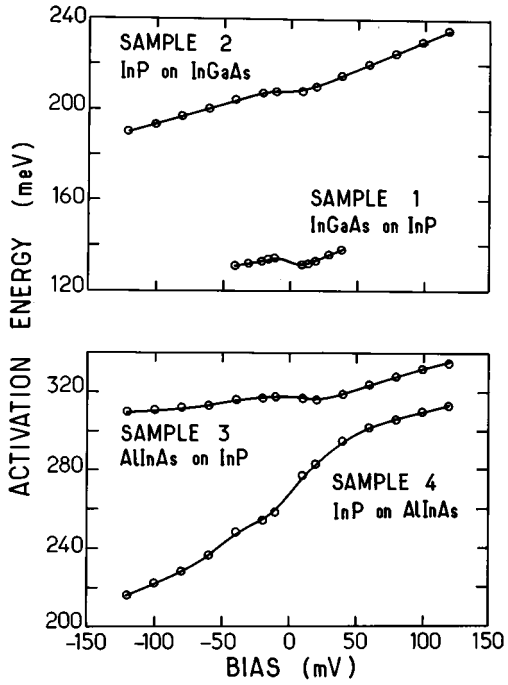

FIG. 3. Activation energies against bias obtained in the four samples under investigation.

duction mechanism. The exponential dependence of the current on the bias implied by Eq. (1) is clearly observed over the experimental range. Incidentally, this result is also in good agreement with numerical simulations of the *JV* characteristics using a diffusion-drift model. The Arrhenius plots [Eq. (2)] derived from these data are shown in Fig. 2(b). Perfect straight line fits (Pearson's confidence ratio $R \geqslant 0.9999$) are obtained for the whole range of voltages and temperatures. The curves obtained with the other samples show qualitatively the same behavior. From the slopes of the Arrhenius plots, we obtain the activation energies $e\phi$ displayed in Fig. 3. As already reported in previous studies[19,20] a weak voltage dependence over the investigated range is observed. A possible explanation could lie in the bias dependence of the barrier form. Interpolation to 0 V yields activation energies of 133 and 209 meV for samples 1 and 2, and 317 and 267 meV for samples 3 and 4, respectively. In order to obtain reliable values of E_0 and E_F, we calculated the charge transfer self-consistently for each sample at the interface as a function of ΔE_c.[21] We assumed the formation of a quasitriangular quantum well in the accumulation layer near the interface and occupation of only the ground level E_0. From the field strength at the interface $F(z=0)$ follows the Schottky lowering ΔE_s:[18]

$$\Delta E_s = \{e^3 F(z=0)/4\pi\epsilon_0\epsilon_r\}^{1/2}. \tag{3}$$

The values for E_0, E_F, ΔE_s, the 2DEG-density n_s, the depletion length L_D, and the resulting CBO's ΔE_c are listed in Table I. We find for the InP-$In_{0.53}Ga_{0.47}As$ system 186 and 272 meV for the direct and inverse interface, respectively, hence a difference of 86 meV. In the InP-$Al_{0.48}In_{0.52}As$ system the asymmetry amounts to 53 meV in the inverse sense with absolute values of 375 and 322 meV for the direct and inverse interface, respectively. As usual, due to several potential error sources the values for the absolute CBO's are not very precise. Temperature dependence of the Fermi level and barrier lowering through Norheim-Fowler tunneling have been neglected. The nominal doping concentrations have not been verified experimentally. Also, one should remember that Eq. (1) is only a crude semiclassical approximation of the underlying physics. We estimate relatively large error bars of ≈40 meV. However, most of the errors inherent to modelization inaccuracies depend weakly on the sample parameters. Thus, they are unimportant as far as offset differences are concerned. The main error source remains the uncertainty on the low-doping concentration, which could vary slightly from sample to sample. For a doubling from 1×10^{16} to 2×10^{16} cm^{-3}, we calculate a change of ΔE_c by ≈10 meV only, which will serve as the error bar for the offset differences.

We also performed additional CBO measurements in the InP-$In_{0.53}Ga_{0.47}As$ samples using the internal photoemission technique.[22,23] Electrons from the $In_{0.53}Ga_{0.47}As$ valence band are optically excited in conduction-band states. When they have enough energy they can overcome the potential barrier into the InP layer. Their accumulation gives rise to a photovoltage U_{ph}. Thus, measuring the photovoltaic re-

TABLE I. Values for E_0, E_F, ΔE_s, L_D, n_s, and ΔE_c obtained from the experimental data associated with self-consistent charge transfer calculations (Ref. 19). The values in parentheses are for internal photoemission. The CBO ratio Q_c is $\Delta E_c/\Delta E_g$, where ΔE_g is the corresponding band-gap difference. Q_c does not make any sense for type-II systems like InP-$Al_yIn_{1-y}As$. Note that the conduction-band effective masses differ by a factor 2 between InP and $In_{0.53}Ga_{0.47}As$.

	Sample 1 $In_xGa_{1-x}As$ on InP	Sample 2 InP on $In_xGa_{1-x}As$	Sample 3 $Al_yIn_{1-y}As$ on InP	Sample 4 InP on $Al_yIn_{1-y}As$
QW	$In_{0.53}Ga_{0.47}As$	$In_{0.53}Ga_{0.47}As$	InP	InP
E_0 (meV)	32.8 (31.6)	38.4 (37.8)	35.5	33.6
E_F (meV)	7.2 (6.8)	9.2 (8.9)	5.9	5.5
ΔE_s (meV)	13.6 (13.2)	15.3 (15.0)	16.9	16.2
n_s (10^{11} cm^{-2})	1.4 (1.3)	1.8 (1.7)	2.2	2.0
L_D (Å)	1420 (1340)	1790 (1740)	2220	2025
ΔE_c (meV)	186 (170)	272 (260)	375	322
Q_c (%)	30.6 (27.9)	44.6 (42.6)		

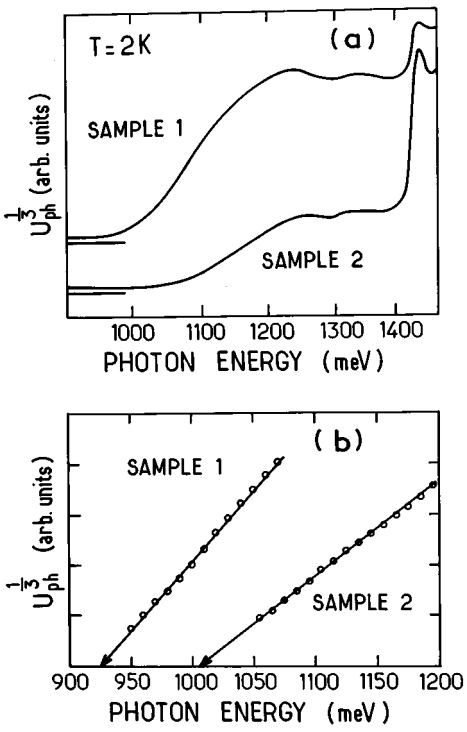

FIG. 4. (a) Photovoltage as a function of the photon energy. (b) Cubic root of the photovoltage U_{ph} versus photon energy. The extrapolation to zero signal yields threshold energies of 925 meV for sample 1 and 1005 meV for sample 2.

sponse as a function of the excitation energy must show a threshold giving a measure for ΔE_c. From Fig. 1(b) we find

$$\Delta E_c = E_T - E_g + E_0 + E_F + E_D + \Delta E_s , \tag{4}$$

where E_T is the threshold energy, E_D is the donor binding energy, and E_g is the $In_{0.53}Ga_{0.47}As$ band-gap energy. The experiments have been performed at $T=2$ K with light from a simple halogen lamp filtered by a grating monochromator and appropriate filters as the excitation source. The photovoltage spectra are shown in Fig. 4(a). For sample 1 we observe an onset at ≈970 meV. The low-background signal below 970 meV can be attributed to intraband absorption by native electrons in the $In_xGa_{1-x}As$ conduction band. The step at 1410 meV originates from electron-hole pairs photogenerated in the InP space-charge region and separated by the built-in electric field. Sample 2 shows the same behavior with an onset at 1050 meV. The stronger InP signal is consistent with the 25% longer InP depletion length (see Table I).

In order to accurately extract the threshold energies from these data, we first subtracted the background signal. Then we followed the conventional approach of internal photoemission,[24] plotting the cubic root of the response U_{ph} versus photon energy. Extrapolation to zero yields the threshold energies of 925 and 1005 meV for samples 1 and 2, respectively, as shown in Fig. 4(b). Using $E_g=810$ meV and $E_D=2.9$ meV,[25] we calculate for the direct and inverse interfaces $\Delta E_c=170$ meV and $\Delta E_c=260$ meV, respectively, thus a difference of 90 meV, which is in nearly perfect agreement with the *JVT* result. These values are indicated in parentheses in Table I. The error sources, linked to inaccuracies of the modelization, remain essentially the same as above. Therefore, we again estimate error bars of 40 meV on the absolute values and much less (around 10 meV) on their differences. The InP-$Al_yIn_{1-y}As$ samples could not be studied with internal photoemission because the threshold energy E_T for a type-II interface is larger than the involved band gaps.

Comparing the present results with available theoretical predictions yields general consistency within the error bars. Our value for the InP-$In_{0.53}Ga_{0.47}As$ asymmetry of some 88 meV is in fair agreement with the 60 meV (in the same sense) calculated by Foulon and Priester.[13] The 180-meV asymmetry reported by Landesman *et al.*[14] is considerably larger but in qualitative accordance. The 53-meV noncommutativity found in InP-$Al_{0.48}In_{0.52}As$ agrees again with the theoretical prediction of Ref. 13 and is in the same sense as the result of Lugagne-Delpon, André, and Voisin,[11] but 50 meV smaller. This quantitative discrepancy is clearly out of the reported error bars. It might reflect a significant difference between their metal-organic chemical-vapor deposition (MOCVD) grown interfaces and our MBE-grown samples. We are inclined to involve the different procedures for commuting the group-V species at the interface. In our case, a 25 s growth interruption is needed to actuate the valves and let the partial pressure of the previous species be negligible. During this growth interruption, phosporus-arsenic exchanges are likely to occur at the sample surface. The number of exchange events is given by a balance between the evaporation rates (which are not negligible for the group-V atoms at the growth temperature) and the impinging fluxes. These effects, when only partial, would tend to symmetrize the direct and inverse interfaces. In the case of the MOCVD-grown samples, the commutation sequence was much shorter (2 s). This could explain the more pronounced offset asymmetry observed by Lugagne-Delpon, André, and Voisin[11] in MOCVD-grown InP-$Al_yIn_{1-y}As$ heterojunctions. Clearly, these exchange mechanisms and their dependence on growth parameters give plausible reasons for a ≈ 50 meV dependence of the measured offsets and offset asymmetry on the growth conditions, especially for no-common atom systems such as those under investigation. That our experimental results compare fairly well with the theoretical results of Ref. 13 may be considered as an indication that the actual interface stoichiometry is not too different from the ideal description. As for the absolute values, they fall within the range of accepted values for both systems. In particular, the properties of narrow quantum wells are sensitive to the average BO value, and the present result for InP-$In_{0.53}Ga_{0.47}As$ (230 meV) agrees quite reasonably with the detailed study of ''double step QW's'' reported by Soucail *et al.* (250 meV).[26] At this point, it is noteworthy that most of the simplifications used in the description of the present experiments lead to a slight underestimate of the actual band offsets.

Checking transitivity in the InP-$Al_yIn_{1-y}As$-$In_xGa_{1-x}As$ family, we find CBO sums of some 500 meV for the $Al_{0.48}In_{0.52}As$-InP-$In_{0.53}Ga_{0.47}As$ growth sequence and some 640 meV for the inverse one. The average sum (570 meV) is significantly larger than the accepted value of 500 meV (Refs. 9 and 27) for the CBO in the $In_{0.53}Ga_{0.47}As$-$Al_{0.48}In_{0.52}As$ system. This nontransitivity of the average band offsets has already been argued by

Lugagne-Delpon, André, and Voisin. Conversely, following Foulon and Priester, transitivity should apply if the proper growth sequence is considered. For instance, the sum of direct InP-$In_xGa_{1-x}As$ and InP-$Al_yIn_{1-y}As$ BO's should equal the $Ga_{1-x}In_xAs$-$Al_yIn_{1-y}As$ BO, and the same result would hold for the sum of the inverse BO's. Our experimental findings are clearly in excellent agreement with this rather particular transitivity rule, which cannot be checked by a direct experiment. Discussion of transitivity properties hence requires some semantic care.

We finally discuss a further qualitative evidence of noncommutativity in the $In_xGa_{1-x}As$-InP system. We consider sample 5 consisting of a MOCVD-grown, 28-period $In_{0.52}Ga_{0.48}As$ (146 Å)-InP(100 Å) superlattice grown on a n^+-type InP (001) substrate. There the direct and inverse interfaces are of course grown in the same ''run'' excluding possible interface differences through varying growth conditions. The residual doping is quite low ($<10^{15}$ cm^{-3}) in this series of samples. Sample structural parameters have been assessed by x-ray double diffraction, giving precise measurement of the layer thicknesses and composition. The PLE spectrum is shown in Fig. 5 and compared with calculated band-to-band absorption spectra for an asymmetrical $In_{0.52}Ga_{0.48}As$-InP quantum well (solid line, 86 meV CBO difference and 250 meV CBO average value) and its symmetrical counterpart (dashed line). The theoretical spectra have been obtained by solving numerically the Schrödinger equation for the envelope functions with a transfer-matrix method, in the potential profiles shown in the inset. Excitonic effects have been neglected. They are expected to introduce corrections in the 3–6 meV range. The much better qualitative agreement of the PLE spectrum with the solid curve is apparent through (i) the ratio of oscillator strengths between the first and second transitions, (''A''$=H1$-$E1$ and ''B''$=L1$-$E1+H2$-$E1$), (ii) the number of absorption steps, which is much larger in the asymmetrical case, and (iii) the band-gap energy itself, which is significantly lowered by ''built-in Stark shift'' and cannot be fitted with the measured layer thickness and composition if a square potential well is assumed. In addition, the quantitative agreement between the PLE spectrum and the solid line, eventually corrected for excitonic effects, is quite satisfactory.

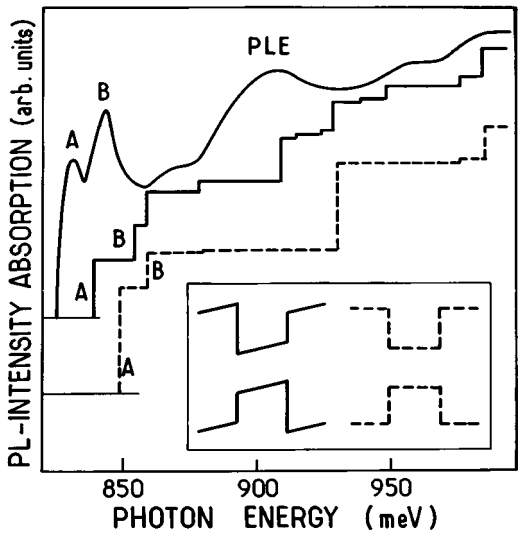

FIG. 5. PLE spectra of sample 5 in comparison with calculated-absorption spectra (i) for an asymmetrical $In_{0.52}Ga_{0.48}As$-InP quantum well (solid line, calculation with an 86-meV CBO difference and a 250-meV CBO average value) and (ii) the symmetrical counterpart (dashed line, calculated using a 250-meV CBO average value). The inset shows the corresponding potential profiles.

In conclusion, we have measured the CBO's of both the direct and inverse interfaces in the InP-$In_{0.53}Ga_{0.47}As$ and InP-$Al_{0.48}In_{0.52}As$ systems. We obtain a 88 ± 10 meV noncommutativity for InP-$In_{0.53}Ga_{0.47}As$, using both the *JVT* and internal photoemission techniques, and 53 ± 10 meV for InP-$Al_{0.48}In_{0.52}As$ using the *JVT* technique. We confirm the significant nontransitivity of the average offsets in the InP-$Al_yIn_{1-y}As$-$In_xGa_{1-x}As$ family of heterostructures. Moreover, our results are in excellent quantitative agreement with the theoretical predictions of Foulon and Priester.

W.S. gratefully acknowledges support accorded by the DAAD Bonn. The MOCVD-grown ''sample 5'' was provided by Dr. J. P. André from Laboratoire d'Electronique Philips. We thank J. C. Hesnault and S. Vuye for their technical help in the device preparation. LPMC-ENS and CNET-Bagneux are ''Unités de Recherche Associées au CNRS.''

*Permanent address: Departemento de Fisica, Universitad Federal de São Carlos, São Carlos, Brazil.

[1] For a comprehensive survey of the question before the age of supercomputing, see *Heterojunction Band Discontinuities: Physics and Device Applications*, edited by F. Capasso and G. Magaritondo (North-Holland, Amsterdam, 1987).

[2] M. A. Haase, M. A. Emanuel, S. C. Smith, J. J. Coleman, and G. E. Stillman, Appl. Phys. Lett. **50**, 404 (1987), and references therein.

[3] J. Tersoff, Phys. Rev. Lett. **56**, 2755 (1986).

[4] M. Cardona and N. E. Christensen, Phys. Rev. B **35**, 6182 (1987).

[5] C. G. Van de Walle, Phys. Rev. B **39**, 1871 (1989).

[6] H. Temkin, K. Alavi, W. R. Wagner, T. P. Pearsall, and A. Y. Cho, Appl. Phys. Lett. **42**, 845 (1983).

[7] K. Imamura, S. Mato, T. Fujii, N. Yokoyama, S. Hiyamizu, and A. Shibatomi, Electron. Lett. **22**, 1148 (1986).

[8] J. R. Waldrop, E. A. Kraut, C. W. Farley, and R. W. Grant, J. Appl. Phys. **69**, 372 (1991).

[9] J. Böhrer, A. Krost, T. Wolf, and D. Bimberg, Phys. Rev. B **47**, 6439 (1993).

[10] M. S. Hybertsen, Appl. Phys. Lett. **58**, 1759 (1991).

[11] E. Lugagne-Delpon, J. P. André, and P. Voisin, Solid State Commun. **86**, 1 (1993).

[12] R. G. Dandrea and C. B. Duke, J. Vac. Sci. Technol. B **10**, 1744 (1992).

[13] Y. Foulon and C. Priester, Phys. Rev. B **45**, 6259 (1992); see also C. Priester, J. Phys. (France) III **1**, 481 (1991).

[14] J. P. Landesman, J. C. Garcia, J. Massies, P. Maurel, G. Jezequel, J. P. Hirtz, and P. Alnot, Appl. Phys. Lett. **60**, 1241 (1992).

[15] This ''macroscopic edge effect'' screening a quantum potential occurs in a variety of physical circumstances, like the ''quantum photovoltaic effect'' [Brum *et al.*, Phys. Rev. B **33**, 1063

(1986), or the built-in piezoelectric field in strained superlattices (Smith and Mailhiot, Phys. Rev. Lett. **58**, 1264 (1987)].

[16] J. M. Moison, F. Houzay, F. Barthe, J. M. Gérard, B. Jusserand, J. Massies, and F. Turco-Sandroff, J. Cryst. Growth **111**, 141 (1991).

[17] T. W. Hickmott, in *Two-Dimensional Systems: Physics and New Devices*, edited by G. Bauer (Springer-Verlag, Berlin, 1986), p. 72.

[18] S. M. Sze, *Physics of Semiconductor Devices* (Wiley, New York, 1981).

[19] J. Batey and S. L. Wright, J. Appl. Phys. **59**, 200 (1985).

[20] J. H. Huang and T. Y. Chang, J. Appl. Phys. **76**, 2893 (1994).

[21] G. Bastard, *Wave Mechanics Applied to Semiconductor Heterostructures* (Les Editions de Physique, Les Ulis, 1988), Chap. V.

[22] G. Abstreiter, U. Prechtel, G. Weimann, and W. Schlapp, Physica B **134**, 433 (1985).

[23] G. Abstreiter, U. Prechtel, G. Weimann, and W. Schlapp, Surf. Sci. **174**, 312 (1986).

[24] J. I. Pancove, *Optical Processes in Semiconductors* (Dover, New York, 1971), p. 287.

[25] *Semiconductors*, edited by O. Madelung, M. Schulz, and H. Weiss, Landolt-Börnstein, New Series, Group III, Vol. 17 (Springer, Berlin, 1982).

[26] B. Soucail, P. Voisin, M. Voos, D. Rondi, J. Nagle, and B. de Crémoux, Semicond. Sci. Technol. **5**, 918 (1990).

[27] Fit of numerous data on $Ga_xIn_{1-x}As$-$Al_yIn_{1-y}As$ quantum wells and superlattices, J. C. Harmand *et al.* (unpublished).